Experimental and Numerical Characterization of the Intra-laminar Fracturing Behavior in Discontinuous Fiber Composite Structures

Seunghyun Ko[1]
Kenrick Chan[1]
Reed Hawkins[2]
Rohith Jayaram[2]
Christopher Lynch[1]
Reda El Mamoune[3]
Minh Nguyen[1]
Nicolay Pekhotin[1]
Natania Stokes[1]
Daniel N. Wu[4]
Mark E. Tuttle[2]
Jinkyu Yang[1]
Marco Salviato[1]

Paper Number: 190

July 11, 2018

ABSTRACT

In this paper, we investigate the intra-laminar size effect of discontinuous fiber composites (DFCs) with three different unidirectional prepreg platelet sizes (75×12, 50×8, and 25×4 mm). Experimentally, we test five different sizes of single edge notched specimens, geometrically scaled (1:2/3:1/3:1/6:1/20), with the constant thickness. We observe notch insensitivity meaning that the crack initiate away from the notch, when the structure sizes are small (from the ratio 1/20 to 1/6). However, the crack always initiate for the ratio of 2/3 and 1. Bazants size effect law is used to analyze such unconventional fracturing behaviors. The experimental results are fitted using the linear regression analysis follow by the size effect law. The transition behavior of the DFCs from the strength based criteria to the energy based criteria is clearly observed. Also, as the platelet size increases, the fracture behaviors shift away from the energy based criteria, which implies a decrease in brittleness. To obtain the intra-laminar fracture energy, G_f, we have developed a finite element model based on the stochastic laminate analogy. The platelet size of 75×12 mm shows 96.8% increase in the fracture energy compared to the platelet size of 25×4 mm while behaves less brittle way. In conclusion, this study examines the effect of the platelet sizes of the DFCs in the presence of the notch. In this process, capturing the quasi-brittleness of the material using the nonlinear fracture mechanics is essential and we accomplish this using the simple size effect law. This work expands on an earlier SAMPE conference proceeding [1], and thus, there is a significant overlap in texts and figures between this and the SAMPE conference proceedings.

[1], Department of Aeronautics & Astronautics, University of Washington, Seattle, WA 98195
[2], Department of Mechanical Engineering, University of Washington, Seattle, WA 98195
[3], Department of Materials Science and Engineering, University of Washington, Seattle, WA 98195
[4], Department of Civil and Environmental Engineering, University of Washington, Seattle, WA 98195

INTRODUCTION

In various sectors industries including aerospace, automobile, and marine engineering, the needs of carbon fiber products with small sizes but complex geometries are growing rapidly. However, using the conventional continuous fiber composites, it is a challenge to fill the needs. The discontinuous fiber composites (DFCs) has an outstanding advantage in the manufacturing of complex structures within a very short period of time compared to the continuous fiber composite [2]. It is made of the platelets or strands that are chopped from the continuous prepreg which can be shaped in complex contours using the closed mold curing method. Therefore, the DFCs open a new opportunity to design complex shapes using carbon fiber composite materials within a short period of manufacturing time.

However, there are still numerous unanswered questions about the DFCs in terms of the relationship between the platelet sizes and material properties, especially under the presence of the notch. From the previous studies [3, 4], the DFCs showed notch insensitivity meaning that the crack can initiate away from the pre-existing notch. However, there are lack of understanding why the DFCs have notch insensitive behaviors. Also, there are only limited amounts of information regarding the fracture property such as the fracture energy of the DFCs.

In this paper, we investigate the fracturing response of the DFCs. We use the size effect test [5] to study the notch insensitivity of the DFCs as well as to find the mode I intra-laminar fracture energy. Also, to study the effect of the platelet sizes, we use three different platelet sizes: 75×12, 50×8 and 25×4 mm. The single edge notch tension (SENT) tests with five different geometrically scaled specimens are used to find the structural size effect in the DFCs. To find the fracture energy, we develop the micro-structure generation algorithm based on the stochastic laminate analogy approach [6, 7, 8].

EXPERIMENT DESCRIPTION

Materials

In order to precisely control the geometry of the platelets, we develop an in-house manufacturing technique of the DFCs. The manufacturing technique is robust enough to vary the size of the platelets as well as to control the thickness of the manufactured plates. A summary of the manufacturing process is in Fig. 1. Detailed explanation is available in [1]. We start with the cutting of two comb-shaped strips from the unidirectional prepreg roll (Fig. 1a). Each strip has the width equal to the platelet width. Then, the combs are separated from each other. We remove the protective backing and cover the surface with a sheet of the parchment paper (Fig. 1b). The silicone coating eases the removal of the paper from the resin after the final cut. We cross-cut the strips to match the length of the platelet (Fig. 1c). The resulting platelets show very accurate dimensions (Fig. 1d). We remove the parchment paper and randomly distribute the platelets into the container (Fig. 1e). The process is repeated until the plate reaches the desired weight (Fig. 1f) to produce consistent

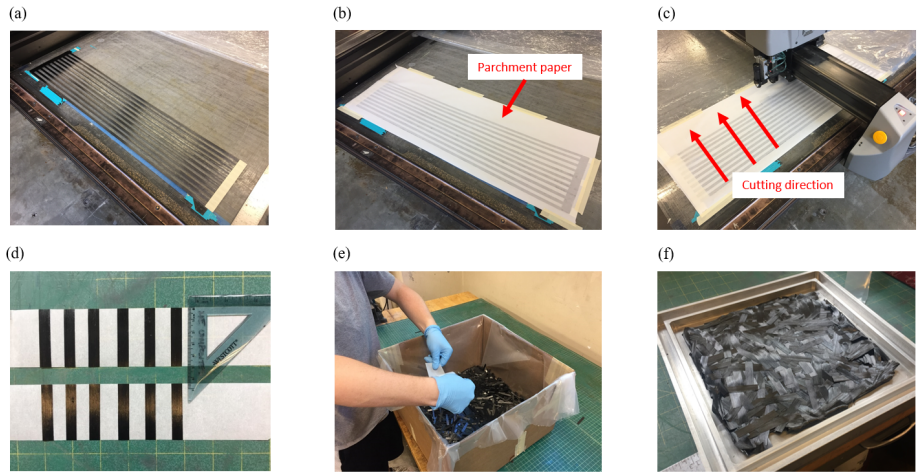

Figure 1. Summary of the in-house manufacturing process of the DFCs.

thickness. To remove the air pockets in between the platelets, We vacuum the plate under 100 kPa for two hours. The plate is ready to be cured using the hot press. The ramping cycle of the hot press is the following: 4.5 °C/min up to 270°C, holds for two hours, and 9 °C/min cools down to the room temperature. Throughout the cycle, we use 0.61 MPa for the pressure. After the cure, the plate is trimmed 15 mm away from the edge using the diamond wet tile saw to discard any uncured regions.

Specimen Characteristics

We prepare five different sizes of the specimens, geometrically scaled in two-dimensions (width and gauge length) with the constant thickness of 3.3 mm (Fig. 2). The largest specimen is referred to as size-1 where the smallest specimen is size-5. All the specimens have an equal ratio between gauge length L, width D, and the initial crack length a_0 (11.125:5:1). The tab length remains the constant. To create a sharp edge notch, we use Zona 35-050 ultra-thin razor saws with 0.2 mm thickness. For the large specimens (size 1 and 2), we use Zona 35-300 medium razor saws with 0.38 mm thickness due to the depth limitation of the ultra-thin saw. The increased thickness of the notch for the large specimens does not have a noticeable impact on the results because the size of the specimen is already large enough compared to the notch thickness.

Experimental Details

We use a servo-hydraulic Instron machine with a 200 kN capacity and a constant crosshead rate. We use the displacement rate of 0.76 mm/min for the largest specimens and linearly scaled the displacement rate for the smaller sizes with respect to the ratio of the width. Each specimen is loaded until final fracture. We measure the load from the Instron machine. The displacement is measured using the digital image correlation technique.

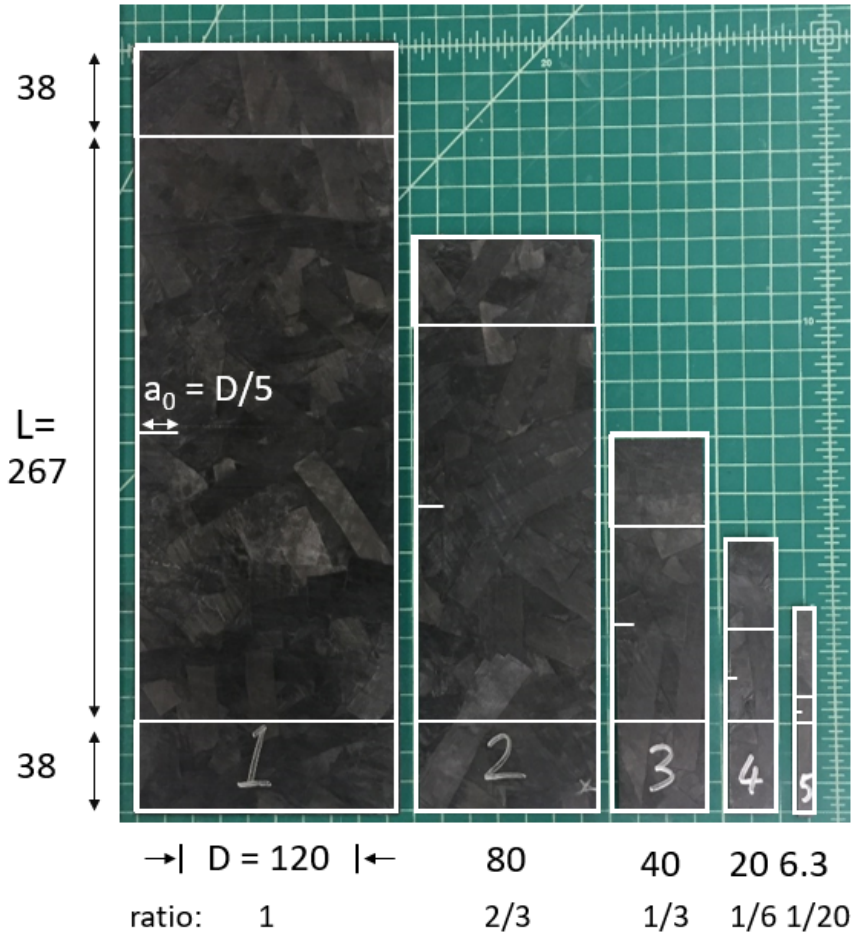

Figure 2. Geometry of scaled SENT specimens. (Units: mm).

EXPERIMENTAL RESULTS

First, we combine the load and displacement curves for the different size of the specimens with the same platelet size. In Fig. 3, typical load-displacement curves for the 75×12 mm platelet size are shown. We can easily recognize the decrease in nonlinearity as the specimen size increases. The slopes of the load-displacement curves become linear for the larger specimen sizes indicating the increased brittleness. The smallest specimen (color pink in Fig. 3) has the strongest nonlinearity before the peak load, indicating the reduced brittleness. This phenomenon implies that the DFCs possess a strong structure size effect. The behavior of the material depends on the structure size.

Second, the fracture surfaces of the DFCs show very distinct characteristic for the different sizes of specimen. The most noticeable feature is that the notch sensitivity indeed depends on the specimen size. Previous studies [3, 4], reported that the DFCs show strong notch insensitive behaviors where the crack initiated away from the notch. We observe the similar notch insensitive behaviors from the specimen size-3, -4, and -5 specimens (Fig. 4a, b). However, as the specimen size increases,

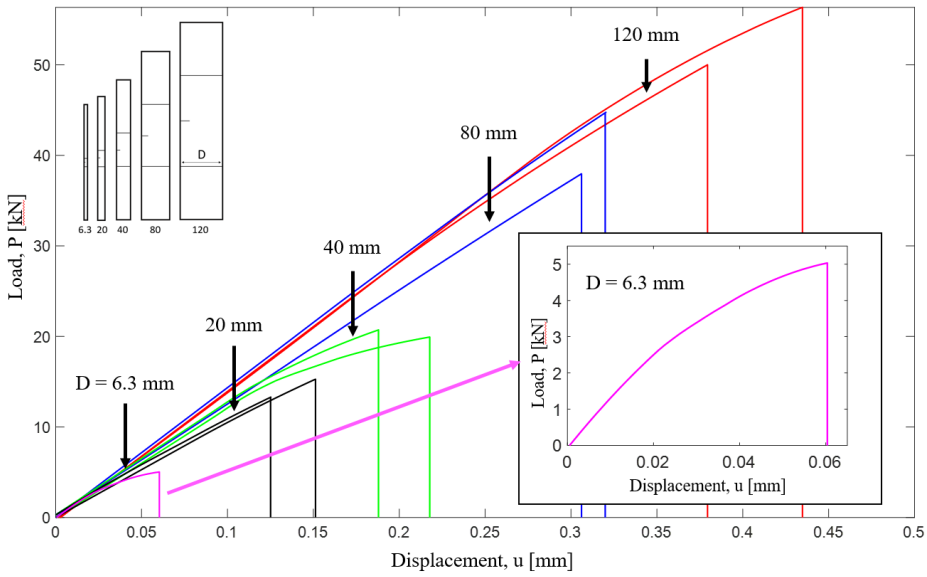

Figure 3. Force and displacement curves for 5 different specimen sizes for the 75×12 mm platelet size, [1].

the notch becomes the dominant factor for the structural failure. For the size-1 and -2, the crack always initiates from the notch. The crack paths are also different for the different specimen sizes. For the small sizes, the path is more chaotic and unpredictable. As the specimen size increases, the path becomes more perpendicular to the loading direction. These findings indicate the stress concentration around the notch becomes the dominant fracture component as the specimen size increases. For the small specimen sizes, the entire gauge area becomes a potential fracture initiation zone. The inherent flaws in the structure such as resin pockets and voids become the important fracture initiation points along with the existing notch. Therefore, we observe the notch insensitivity from the small specimen sizes only.

The SENT results are summarized in Fig. 5. We define the nominal strength as the average stress at the failure within the un-notched cross-sectional area. The test results certainly show the decreasing trend of the nominal strength with the increasing specimen size in all platelet sizes. If we try to explain this trend in terms of the strength-based failure criteria such as Tsai-Wu or Tsai-Hill, it is not so intuitive to do. Furthermore, linear elastic fracture mechanics (LEFM) is not sufficient enough to explain the decreasing strength because according to the LEFM, the strength should decrease linearly proportional to $D^{-1/2}$. However, we find the nominal strengths remain stagnant in small width cases. Therefore, we use Bazants size effect law (SEL) [9] to analyze the test results of the DFCs.

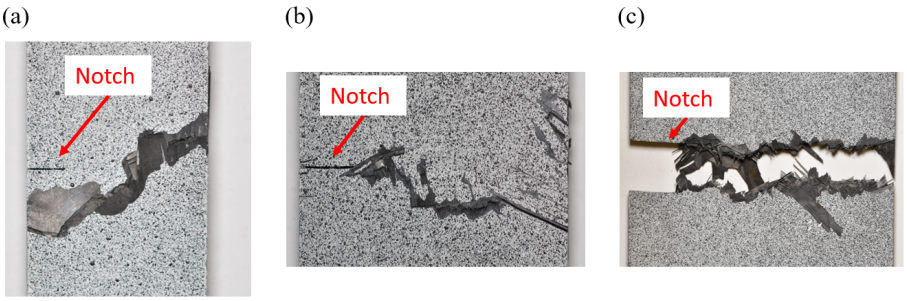

Figure 4. Fracture surfaces of the 50×8 mm platelet size specimens. (a) D = 20 mm showing notch insensitive, (b) D = 40 mm, (c) D = 120 mm

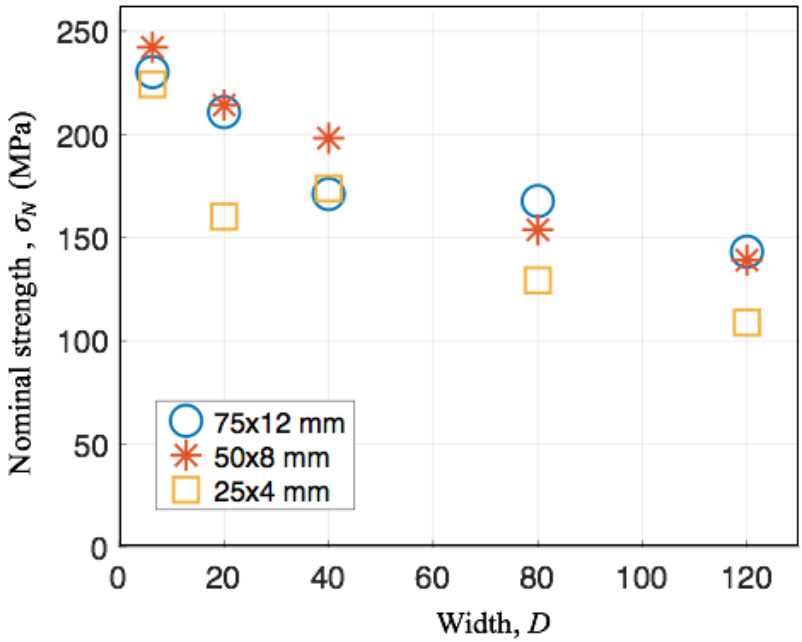

Figure 5. Average nominal strength for the different specimen sizes and the platelet sizes of the DFCs.

DISCUSSION

Analysis using Size Effect Law (SEL)

We use Bazants type II SEL [9] to analyze the experimental results. The SEL relates the nominal strength, σ_N in terms of the characteristic size of the structure. For this study, we choose the width of the specimen, D as the characteristic size. We adopt the equivalent linear elastic fracture mechanics approach to relate σ_N with D using the material properties (fracture energy, G_f and effective fracture process zone (FPZ) length, c_f and the geometry properties (dimensionless energy release rate $g(\alpha)$ and $g'(\alpha)$). Starting with the LEFM, the energy release rate in terms of the relative

crack length can be expressed as follow:

$$G(\alpha) = \frac{\sigma_N^2 D}{E^*} g(\alpha) \tag{1}$$

We define the parameters used in Eq. 1 such that α = a/D, normalized effective crack length where a is the crack length, σ_N = $P/(Db)$ where P is the load applied, b is the thickness, $E*$ = E for the plane stress and $E/(1-\mu^2)$ for the plane strain, and $g(\alpha)$ = dimensionless energy release rate. The length of the crack at the failure can be written using an effective crack length $a = a_0 + c_f$ where a_0 = initial crack length and c_f = effective FPZ length which is assumed to be the material property. Substituting this into Eq.1, we can define the fracture energy, G_f, in terms of the effective crack length:

$$G_f = G(\alpha_0 + \frac{c_f}{D}) = \frac{\sigma_N^2 D}{E^*} g(\alpha_0 + \frac{c_f}{D}) \tag{2}$$

In this particular study G_f is the mode I intra-laminar fracture energy of the material. By approximating the $g(\alpha)$ with the Taylor expansion at α_0 and only keeping the linear term, we have the following expression for G_f:

$$G_f = \frac{\sigma_N^2 D}{E^*} [g(\alpha_0) + \frac{c_f}{D} g'(\alpha_0)] \tag{3}$$

Here, $g'(\alpha_0)$ = $\partial g(\alpha_0)/\partial\alpha$. Rearrange the Eq. 3, we express the nominal strength in terms of the material properties, and the structure size D.

$$\sigma_N = \sqrt{\frac{E^* G_f}{D g(\alpha_0) + c_f g'(\alpha_0)}} \tag{4}$$

Equation 4 is simplified to match the size effect law.

$$\sigma_N = \frac{\sigma_0}{\sqrt{1 + D/D_0}}, \text{ where } \sigma_0 = \sqrt{\frac{E^* G_f}{c_f g'(\alpha_0)}} \text{ and } D_0 = c_f \frac{g'(\alpha_0)}{g(\alpha_0)} \tag{5}$$

σ_0 and D_0 are the constant values depending on the FPZ size and the specimen geometry for homogeneous material [9]. However, the DFC is non-homogeneous material due to the complex micro-structure. Therefore, a series of $g(\alpha_0)$ and $g'(\alpha_0)$ are computed using the finite element model to obtain the average values of $g(\alpha_0)$ and $g'(\alpha_0)$. The averaged values are relatively close to each other within 10% of coefficients of variation, meaning that the SEL still holds for the DFCs. Equation 5 presents the dependency of the nominal strength in terms of the structure size D. Unlike the classical LEFM where the nominal strength is linearly proportional to $D^{-1/2}$, Eq. 5 includes the characteristic length D_0. This characteristic length allows the SEL to describe the change in structural response from ductile to brittle as the structure size increases.

Fitting of Experimental Data by Size Effect Law

To obtain the SEL parameters, we define the following terms:

$$X = D,\ Y = \sigma_N^{-2} \tag{6}$$

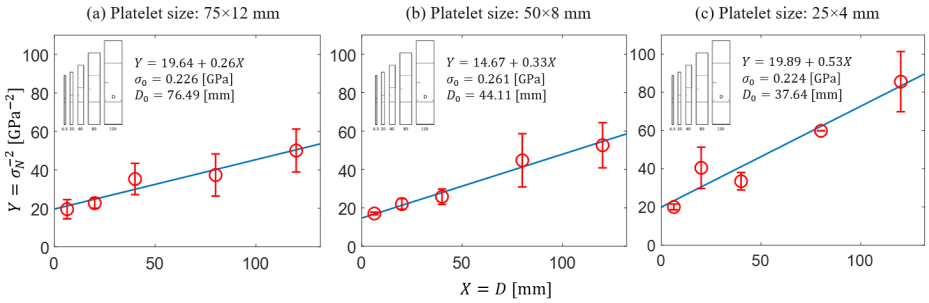

Figure 6. Linear regression analysis of the experimental results for the platelet size of (a) 75×12 mm, (b) 50×8 mm, and (c) 25×4 mm.

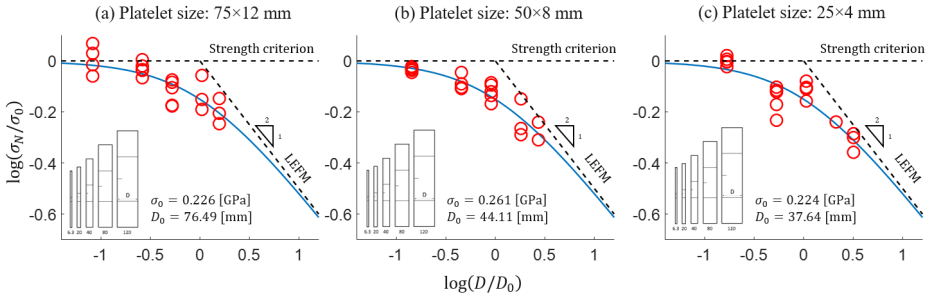

Figure 7. Size effect curves for the platelet size of (a) 75×12 mm, (b) 50×8 mm, and (c) 25×4 mm.

$$\sigma_0 = C^{-1/2},\ D_0 = \frac{C}{A} = \frac{1}{A(\sigma_0)^2} \tag{7}$$

The SEL is expressed in a simple linear form combining Eq. 6 with 7:

$$Y = AX + C \tag{8}$$

To construct the size effect curve, we obtain the SEL parameters using Eq. 7 (see Fig. 6). Using the parameters, we can plot the size effect curves (see Fig. 7). For the platelet size of 75 × 12 mm, σ_0 = 0.226 GPa and D_0 = 76.49 mm. For the platelet size of 50 × 8 mm, σ_0 = 0.261 GPa and D_0 = 44.11 mm. For the platelet size of 25 × 4 mm, σ_0 = 0.224 GPa and D_0 = 37.64 mm. The characteristic length, D_0 significantly affected by the platelet sizes. As the platelet size decreases, the characteristic length also decreases implying enhanced brittleness of the structure response. Next, we construct the size effect curve using the size effect parameters with Eq. 5 on Fig. 7 where the normalized nominal strength σ_N/σ_0 is plotted as a function of the normalized characteristic size D/D_0 in a double logarithmic scale. A horizontal asymptote represents the strength criteria where there is no size effect or length dependent. An asymptote line with a slope of -1/2 represents the LEFM where the strongest size effect exists. The intersection point where two asymptotes meet (D = D_0) represents the transition size where the structure behavior changes from one to other.

There are two important observations from Fig. 7. (1) The failure of the DFCs

containing the traction-free notch expresses a strong size effect. The experimental data fit well with the size effect law. (2) The platelet size has a strong influence on the fracturing behavior of the DFCs. The larger platelet size shows more ductile response whereas the smaller platelet size exhibits a more brittle response. Also, using the SEL, we can explain why some of the previous studies [3, 4] observed notch insensitive fracturing behavior of the DFC. If the structure size is small enough that the FPZ size becomes comparable with the characteristic length, D, the material behaves notch insensitive. Therefore, the relative size of the structure and the FPZ must be taken into account when we analyze the failure of the DFCs.

DEVELOPMENT OF STOCHASTIC FINITE ELEMENT MODEL

Unlike the conventional continuous fiber composite, the DFCs possess unique micro-structure made of randomly distributed platelets. Therefore, the micro-structure of the DFCs have to be explicitly simulated in order to capture the global response of the material. To generate the micro-structure, we develop a 2D finite element model using the stochastic laminate analogy. The stochastic laminate analogy divides the structure into multiple partitions, apply stochastic distributions of the platelet layups, and analyze the partitions as a homogeneous laminate using the classical laminate theory [10]. Feraboli et al. [6] and Harban et al. [7] applied the analogy to the DFCs, simulate the material properties such as the in-plane ultimate strength and the in-plane modulus. Selezneva et al. [8] stepped further more by explicitly generated the platelets with random orientations and locations within the given space. This method generated a smooth transition of the local stiffness between adjacent partitions which in result provided a more accurate imitation of the DFCs morphology. We adopt Seleznevas model and further improved it by adjusting the thickness of the partitions by including the resin layers.

Micro-structure Generation Algorithm Scheme

The randomly oriented platelets are generated using Matlab. The algorithm randomly chooses a central location and the orientation of the platelet. We apply the normal distribution for statistical variations but any statistical variations can easily be adapted. Figure 8 presents a basic morphology of the platelet on top of the partitions. If a part of the platelet goes beyond the structure, it simply trims the outside part. Each platelet generation checks the average number of platelets through the thickness. The platelet generation stops after the average number of platelet within the structure reaches the target platelet average. The target platelet average is equal to the total thickness divided by the platelet thickness. For 3.3 mm thickness, the target platelet average is equal to 24. Due to the random distribution of the platelets, each partition has a different number of platelets through the thickness. Since each partitions total thickness is set to be uniform, the individual ply thickness needs to be adjusted accordingly. When the number of platelets through the thickness reached beyond the target platelet average, ply thickness decreased linearly to match the target thickness. However, when it is lower than the target, linearly increasing the thickness

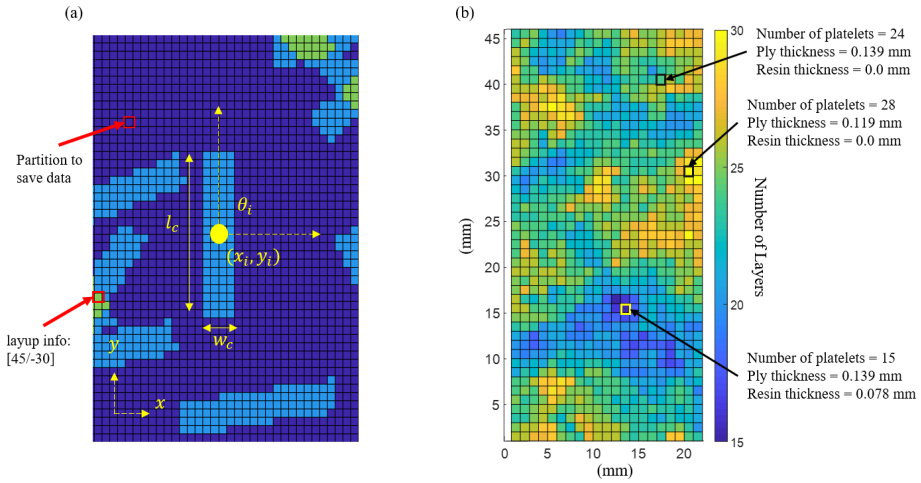

Figure 8. Generation of micro-structure of the DFCs (a) basic platelet morphology, (b) constructed micro-structure after thickness adjustment and resin inclusion, [1].

of the plies are not realistic. Instead, we insert resin layers in between the plies to match the target thickness. The resin layers have isotropic properties equal to the matrix, therefore, the total stiffness of the structure is not significantly affected by the inclusions.

Another key feature that we developed is the controlled platelet distribution algorithm. As we mentioned before, there are stochastic variations in the number of platelets through the thickness in the partitions. In certain regions, the number of average platelets is extremely low or extremely high, causing an unrealistic representation of the DFCs. These unrealistic representations are caused by uncontrolled depositions of the platelets in a given space. First, we control the shortage of platelets using the stopping points (called saturation points) on the average number of platelets through the thickness. The platelet generation scheme can only pass the saturation points when the average number of platelets meet the saturation points or a certain number of iterations is passed without any further deposition (Fig. 9a). The saturation points force the platelet generation scheme to find the locations of the unrealistic shortage of platelets in the geometry. Second, to limit the unrealistic concentrations of the platelets, we restrict the deposition of the platelets in certain partitions if they reach the maximum possible average number of platelets. The maximum number is chosen based on the microscope observations. We count the total of 90 different cross-sections of the DFC samples. The coefficient of variation for the number of platelets through the thickness is 0.22. Therefore, the maximum number of platelets through the thickness is set to be 29. This causes the mild skewed distribution of platelets through the thickness (Fig. 9b). The summary of the micro-structure generation algorithm is summarized in Fig. 11.

Find $g(\alpha)$, $g'(\alpha)$, and Intra-laminar Fracture Energy, G_f.

After the micro-structure is generated, the partitions are transferred to Abaqus/Standard. Abaqus imports the individual platelet orientation and thickness, build sets of lami-

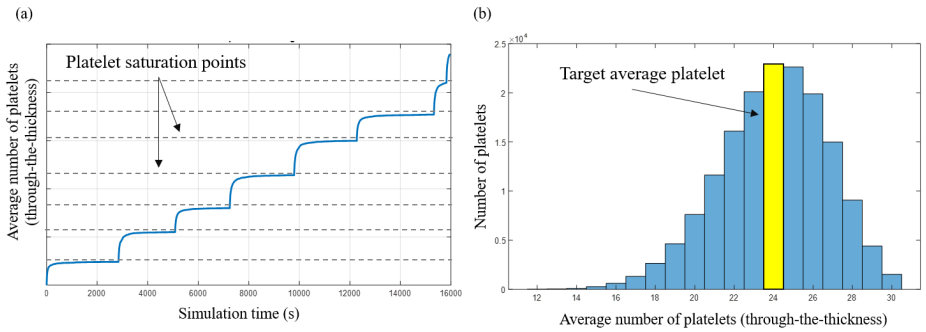

Figure 9. Platelet distribution algorithm. (a) saturation points to prevent the platelet shortages, (b) controlled distribution of the platelets, [1].

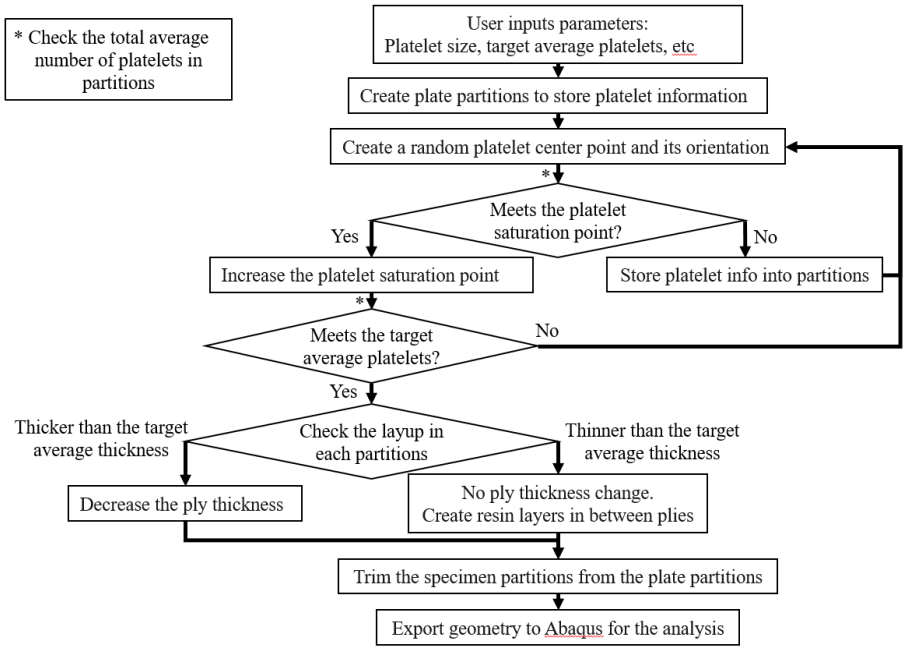

Figure 10. Flow chart of the micro-structure generation algorithm.

nates. We use eight-node shell elements (S8R) for the analysis. The simplest way to find the value of $g(\alpha)$ and $g'(\alpha)$ is J-integral approach. However, the method does not work for the DFCs because of inhomogeneous material characteristics. Therefore, we use following expression:

$$G(u,a) = \frac{-1}{b}\left[\frac{\partial \Pi(u,a)}{\partial a}\right]_u \tag{9}$$

In Eq. 9, u is the equilibrium displacement, b is the thickness, a is the crack length, and Π is the potential energy. We obtain the series of potential energy or internal energy of the entire structure from Abaqus by increasing the crack length but keeping the constant displacement. Using the central difference scheme, we obtain $G(\alpha)$. Then, we calculate $g(\alpha)$ using Eq. 10:

$$g(\alpha) = \frac{G(\alpha)E^*}{\sigma_N^2 D} \tag{10}$$

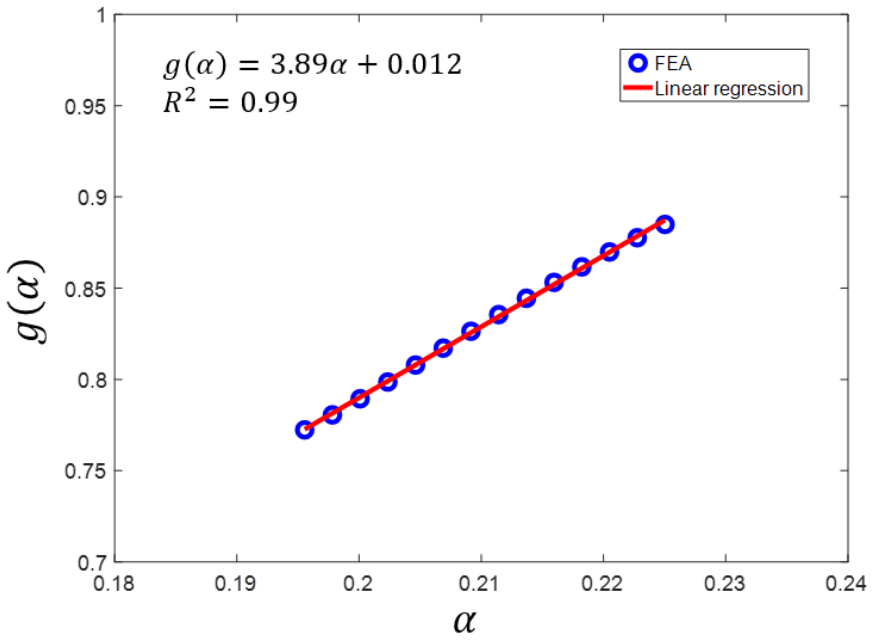

Figure 11. The simulated results of the dimensionless energy release rate $g(\alpha)$ for platelet size of 50×8. g'(α) is calculated using the linear regression analysis.

TABLE I. MEASURED FRACTURE PROPERTIES OF THE DFCS WITH PLATELET SIZE OF 75×12, 50×8, AND 25×4 MM. (THICKNESS IS 3.3 MM)

Platelet size (mm)	$g(\alpha_0)$	$g'(\alpha_0)$	Fracture energy G_f (N/mm)	Effective FPZ length c_f (mm)
75×12	0.88±0.03	4.79±0.67	65.98±2.8	14.16±1.85
50×8	0.93±0.11	5.60±0.75	53.72±6.14	7.43±0.83
25×4	0.93±0.07	5.51±1.2	33.59±2.86	6.55±1.07

Figure 11 shows an example of $g(\alpha)$ for a single specimen. The values of $g(\alpha)$ and $g'(\alpha)$ deviates for different micro-structure. To get an average value, we simulate 10 specimens on each platelet sizes. Finally, we calculate the fracture energy G_f and the effective FPZ length c_f for the DFCs with 75×12, 50×8, and 25×4 mm platelet sizes with 3.3 mm thickness (see Table I). The fracture energy G_f and the effective FPZ length c_f show significant differences between the three platelet sizes. G_f increases by 96.8% when the platelet size ratio increased by three times. Also, the length of the effective FPZ size increases as the platelet size increases. As the size of the FPZ increases, the material response deviates from the LEFM. This explains the ductile behavior of the DFCs with larger platelet sizes.

CONCLUSION

In this study, we investigate and discuss the intra-laminar size effect of the DFCs with three different platelet sizes (75×12, 50×8 and 25×4 mm). From the experi-

mental results of the geometrically-scaled single edge notch tension specimens, we observe a strong structure size effect in the DFCs. The fracturing behavior of the DFCs shows a smooth transition from ductile to brittle depending on the structure size. Also, the intensity of the quasi-brittleness in the DFCs depends strongly on the platelet size. We observe that having a larger platelet size (75×12 mm) makes the structure behaves in more ductile manner. The DFCs with a smaller platelet size (25×4 mm) fractures in a more brittle manner. We obtain the initial intra-laminar mode I fracture energy G_f and the effective fracture process zone (FPZ) length c_f for the DFCs using the size effect tests and the finite element analysis. The finite element model provides the dimensionless energy release rate. The G_f of the DFCs with 75×12 mm platelet size shows 96.8% increase compare with the 25×4 mm platelet size DFCs. We conclude that along with the structure size effect, the DFCs also has the platelet size effect. By changing the size of the platelet, we can engineer the fracture energy of the DFCs.

ACKNOWLEDGEMENTS

We acknowledge the financial support by the FAA-funded Center of Excellence for Advanced Materials in Transport Aircraft Structures (AMTAS) and The Boeing Company. We thank the project monitors for their support and guidance: Ahmet Oztekin, Cindy Ashforth, and Larry Ilcewicz from the FAA, and William Avery from the Boeing Company. We thank Professor Anthony Waas from the University of Washington for letting us use his experimental equipment. We also thank technical support provided by Bruno Boursier from the Hexcel Corporation, Bill Kuykendall, and Michelle Hickner in Mechanical Engineering at the University of Washington.

REFERENCES

1. Ko, S.,Chan K., Hawkins R., Jayaram R., Lynch C., El Mamoune R., Nguyen M., Pekhotin N., Stokes N., Wu D., Yang J., Tuttle M., and M. Salviato. 2018. Characterization and computational modeling of the fracture behavior in discontinuous fiber composite structures, SAMPE Conference, 2018. The present conference proceeding is more comprehensive than this SAMPE one in that we have newly added experimental results on 25×4 mm platelet size results to complete the size effect study.

2. Boursier, B. 2001. New possibilities with HexMC, a high performance moulding compound, 22nd SAMPE European conference, March 2001.

3. Boursier, B., and A. Lopez. 2010. Failure initiation and effect of defects in structural discontinuous fiber composites, SAMPE. Seattle, Washington, 2010.

4. Feraboli, P., Peitso, E., Cleveland, T., Stickler, P., and J. C. Halpin. 2009. Notched behavior of prepreg-based discontinuous carbon fiber/epoxy systems, Comp. Part A. 40 (2009) 289-299.

5. Salviato, M., Kirane, K., Ashari S.E., Bazant, Z.P., and G. Cusatis. 2016. Experimental and numerical investigation of intra-laminar energy dissipation and size effect in two-dimensional textile composites, Comp. Sci. and Technol. 135 (2016) 67-75.

6. Feraboli, P., Cleveland, T., Stickler, P., and J. Halpin. 2010. Stochastic laminate analogy for simulating the variability in modulus of discontinuous composite materials, Comp. Part A. 41 (2010) 557-570.

7. Harban K., and M. Tuttle. 2017. Reducing certification costs of discontinuous fiber composite structures via stochastic modeling, U.S. Department of Transportation Federal Aviation Administration, May 2017.

8. Selezneva, M., Roy, S., Meldrum, S., Lessard, L., and A. Yousefpour. 2017. Modelling of mechanical properties of randomly oriented strand thermoplastic composites, J. of Comp. Mat., 51 (2017), 831-845.

9. Bazant, Z.P., Daniel, I.M., and Z. Li. 1996. Size effect and fracture characteristics of composite laminates, J. Eng. Mater. Technol. 118 (3) (1996) 317-324.

10. Halpin, J.C., and N.J. Pagano. 1969. The laminate approximation for randomly oriented short fiber composites, J. of Comp. Mat., vol.3 (1969), 70.